



DOI: 10.18720/MCE.91.8

## Equilibrium finite elements for plane problems of the elasticity theory

**Yu. Ya. Tyukalov**

*Vyatka State University, Kirov, Russia*

\* E-mail: [yutvgu@mail.ru](mailto:yutvgu@mail.ru)

**Keywords:** stress approximations, additional energy, finite element method, plane problem

**Abstract.** The work is devoted to the finite elements construction, based on the stresses approximation, for solving plane problems of the elasticity theory. Such elements are alternative to existing finite elements obtained using displacements approximation. Alternative solutions allow more accurate assessment of the structure stress-strain state. The proposed method for constructing finite elements is based on the principles of minimum additional energy and possible displacements. Various stress approximation variants are considered. All approximations variants satisfy the differential equilibrium equations for the case of no distributed load. A comparison is made of the solutions which are obtained by the proposed method with analytical solutions for the ring and the bent beam. The considered stress approximation variants show for test problems good accuracy and convergence, when we grind finite elements grid. It is shown that the best accuracy in calculating stresses and displacements is provided by the finite element with piecewise constant approximations of stresses. In addition, such finite element ensures the displacements convergence to exact values from above. Other finite element variants may be convenient for calculating branched and combined structures. The proposed equilibrium finite elements can be used to more accurately determine the stresses in the calculated structures. The proposed technique can be used to build volumetric finite elements.

### 1. Introduction

To the basics of the finite element method large number of fundamental studies are devoted, for example papers [1, 2]. These present various variational principles, based on which, finite element solutions can be constructed for the wide range of structural design problems. Alternative principles of minimum potential energy and additional energy are considered. In addition, various variants of hybrid and mixed variational principles are studied. It is noted that the solutions based on the principle of minimum potential energy make it possible to obtain, under certain conditions, the lower limit of displacements, and those obtained using the principle of additional energy can provide the upper limit of displacements. It is obvious that by applying various approximations for displacements in the area of finite element, we thereby forcefully reduce the number of system freedom degrees, which leads to an increase its rigidity [3]. Therefore, the values of displacements determined by the finite element method in displacements will always be less of accurate values. In addition, as rule, the approximations used for displacements do not ensure the deformations continuity, and hence the stresses continuity, along the finite element boundaries. This leads to the appearance of stress field discontinuities along the finite element boundaries.

The finite element method is successfully used to solve various geometrically and physically nonlinear problems. It successfully used for calculating rods, plates, shells and volume problems of the elasticity theory [4, 5]. The finite element method is widely used to solve problems with geometric nonlinearity, shear deformations and for calculation thin-walled structures. The finite element method in displacements is the universal method for solving various problems of the construction's stability and dynamics [6, 7].

The papers [8, 9] are devoted to mixed variants of the finite element method. In mixed methods, approximations of both displacements and stresses (forces) are used. In [9], to approximate displacements and stresses, low-order functions are used. Then two numerical examples are given to demonstrate the

---

Tyukalov, Yu.Ya. Equilibrium finite elements for plane problems of the elasticity theory. Magazine of Civil Engineering. 2019. 91(7). Pp. 80–97. DOI: 10.18720/MCE.91.8

Тюкалов Ю.Я. Равновесные конечные элементы для плоских задач теории упругости // Инженерно-строительный журнал. 2019. № 7(91). С. 80–97. DOI: 10.18720/MCE.91.8



This work is licensed under a [CC BY-NC 4.0](https://creativecommons.org/licenses/by-nc/4.0/)

stability and efficiency of the proposed approach. The solution obtained by the mixed method, when crushing the finite element's grid, can approach the exact solution both from the bottom and from the top and does not give any lower or upper boundaries of displacements [10, 11].

As an alternative to the finite element method in displacements, for certain structure's types, numerical methods are used, which based on the decomposition of the displacement function into trigonometric series [12,13]. Such methods allow obtaining high-precision solutions for the certain class of problems and can use to testing of other numerical methods.

Also, the boundary element method which use boundary displacement approximations is applied to calculate various constructions [14, 15]. In [16], solutions of three-dimensional problems of the elasticity theory near the border are investigated using modern computational technologies. In [17] for the analysis of axisymmetric elastic problems, the new hybrid finite element method was proposed. This technique uses fundamental solutions in combination with boundary integration method. The formulation uses two independent displacement fields. One field is used within the region of the element and the second is used on the element border, that combines the advantages of the traditional methods of finite and boundary elements. In [18], the Galerkin's method in the weak form is used to reduce the approximating function orders.

In [19, 20], finite element solutions were developed based on stress (force) approximations. At the same time, to build the solution the combination of principles of the minimum additional energy and the possible displacements was used. Such approach makes it possible to find solutions that are alternative of solutions obtained by the finite element method in displacements. It is known, the finite element method in displacements gives an approximate and one-sided solution of the problem. Therefore, despite the great success in using the finite element method in displacements, the search and development of additional, and alternative solutions are relevant. Alternative solutions make it possible to obtain the necessary assessment of the solutions accuracy, which obtained by the finite element method in displacements, and thus ensure the adoption of more reliable design solutions. In [21, 22], this approach is used to solve stability problems and free oscillations of rod systems.

This work aim is to develop the method to solve the flat elasticity problems, which is based on various variants of stress approximations at finite element region. In this case, it is supposed to use various options for approximating stresses that satisfy homogeneous differential equilibrium equations in the finite element region. The method using stress approximations is an alternative to the standard, widely used, finite element method, which is based on the displacement approximations. The flat elasticity theory problems are encountered at the calculations of wide range of the modern building structures. Therefore, the improvement of their solution methods remains the urgent task.

## 2. Methods

The solution of the theory elasticity problems in stresses can be obtained based on the additional energy functional [1, 2]:

$$\Pi^c = \frac{1}{2} \iint \{\sigma\}^T [E]^{-1} \{\sigma\} d\Omega - \int \{T\}^T \{\bar{\Delta}\} dS \rightarrow \min. \quad (1)$$

$\{\bar{\Delta}\}$  is the vector given displacements of nodes;

$\{T\}$  is the vector boundary forces;

$S$  is the boundary surface, on which the displacement nodes are given;

$\Omega$  is the subject area;

$\{\sigma\}^T = (\sigma_x \quad \sigma_y \quad \tau_{xy})$  is the stresses vector;

$[E]$  is the material stiffness matrix.

We shall obtain the necessary relations for an arbitrary quadrangular finite element (Figure 1). In Figure 1, points  $A, B, C, D$  are located on the middles of corresponding sides.

To approximate stresses over the finite element region, we shall use functions that satisfy homogeneous differential equilibrium equations for the plane elasticity theory problem:

$$\frac{\partial \sigma_x}{\partial x} + \frac{\partial \tau_{xy}}{\partial y} = 0, \quad \frac{\partial \sigma_y}{\partial y} + \frac{\partial \tau_{xy}}{\partial x} = 0. \quad (2)$$

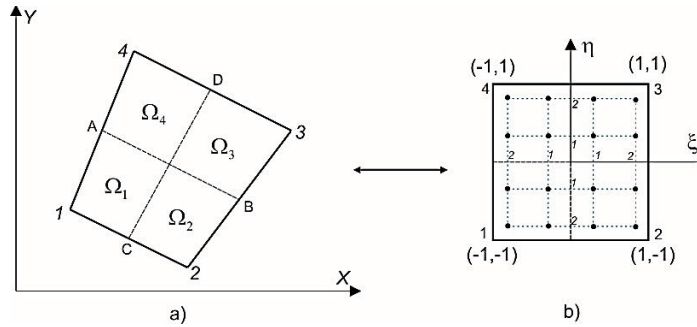


**Figure 1. Converting an arbitrary quadrangular finite element into the square.**  
**a) areas with constant stresses for variant 4;**  
**b) points 1, 2 on the axes are the points for numerical integration on Gauss.**

To compare the solutions, we shall use four variants of approximating functions, which are presented in Table 1.

**Table 1. Variants of the approximating functions for the stresses.**

Variant	$\sigma_x$	$\sigma_y$	$\tau_{xy}$
1	$a_1 + a_4 y + a_6 x$	$a_2 + a_5 x + a_7 y$	$a_3 - a_6 y - a_7 x$
2	$a_1 + a_4 y$	$a_2 + a_5 x$	$a_3$
3	$a_1 + a_6 x$	$a_2 + a_7 y$	$a_3 - a_6 y - a_7 x$
4	$\sigma_{x,i}, (x, y) \in \Omega_i$	$\sigma_{y,i}, (x, y) \in \Omega_i$	$\tau_{xy,i}, (x, y) \in \Omega_i$

Variants 2 and 3 are obtained from variant 1 by eliminating some unknown parameters. All the approximation functions satisfy equations (2). In variants 1–3, the unknown parameters  $a_1 \div a_7$  are independent for each finite element; therefore, the stress fields will have discontinuities along the finite elements' boundaries. Variant 4 uses piecewise constant functions  $\sigma_{x,i}, \sigma_{y,i}, \tau_{xy,i}$  that are nodal stress values. Thus, stresses are approximated by constant functions in each region  $\Omega_1 \div \Omega_4$  of the finite element (Figure 1a). Such stress fields are continuous at nodes and along the finite elements boundaries but have discontinuities inside the elements. Such approximations for rectangular and triangular finite elements are used in [19–22].

For the stress fields to satisfy the equilibrium equations for the entire subject area under the given load action, we construct the equilibrium equations for finite element grid nodes. For that we shall use the possible displacements principle. The unit displacements along the coordinate axes (Figure 2) are taken as possible displacements. In this case, only finite elements that are adjacent to the node are will deformed.

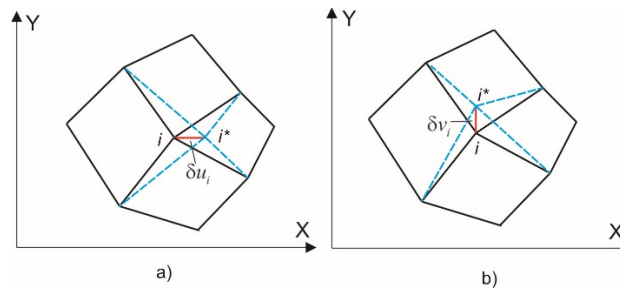


**Figure 2. Possible displacements of node i.**

Such equilibrium equations can be written as follows:

$$\begin{aligned} \{C_{i,x}\}^T \{\sigma_i\} + \bar{P}_{i,x} &= 0, \quad i \in \Xi_x, \\ \{C_{i,y}\}^T \{\sigma_i\} + \bar{P}_{i,y} &= 0, \quad i \in \Xi_y. \end{aligned} \tag{3}$$

$\{\sigma_i\}$  is the unknown parameters vector of stresses for finite elements that are adjacent to node  $i$ ;

$\Xi_x, \Xi_y$  are the sets of nodes that have loose displacements along the  $X$  and  $Y$  axes, respectively;

$\bar{P}_{i,x}, \bar{P}_{i,y}$  are the generalized forces corresponding to the external loads potential on single possible displacements of the node  $i$ , which are directed along the axes  $X, Y$ ;

$\{C_{i,x}\}, \{C_{i,y}\}$  are the vectors containing coefficients for unknown nodal stress parameters in the equilibrium equations of node  $i$ .

Using any variant of the approximating functions (Table 1), the expression of the functional (1), when the given displacements are absent, can be written in the following matrix form:

$$\Pi^c = \frac{1}{2} \{\sigma\}^T [D] \{\sigma\} \rightarrow \min. \quad (4)$$

The matrix  $[D]$  is the flexibility matrix of the entire system. Thus, we have obtained the problem of the quadratic function minimizing (4) with constraints, which are represented as the system of linear algebraic equations (3). Using for solving the Lagrange's multipliers method, we shall get the following extended functional:

$$\Pi^c = \frac{1}{2} \{\sigma\}^T [D] \{\sigma\} + \sum_{j=x,y} \sum_{i \in \Xi_j} u_{i,j} \left( \{C_{i,j}\}^T \{\sigma_i\} + \bar{P}_{i,j} \right) \rightarrow \min, \quad (5)$$

$u_{i,j}$  is the displacement of node  $i$  in direction  $j$ . With this solution, additional unknowns appear in the form of nodes displacements. But we must accent, that displacements fields approximations in the finite element region are not used.

Expression (5) can be represented in the more convenient to solve form:

$$\Pi^c = \frac{1}{2} \{\sigma\}^T [D] \{\sigma\} + \{u\}^T (\{F\} - [L] \{\sigma\}) \rightarrow \min, \quad (6)$$

$\{u\}$  is the global vector of unknown nodal displacements;

$\{F\}$  is the vector whose elements are equal to the works of external forces on the corresponding single displacements;

$[L]$  is the "equilibrium" matrix, the rows of which are formed from the corresponding vectors  $\{C_{i,j}\}$ .

If we equate to zero the derivatives with respect to the vectors  $\{\sigma\}$  and  $\{u\}$ , we obtain the following algebraic equations system:

$$\begin{bmatrix} [D] & -[L]^T \\ -[L] & [0] \end{bmatrix} \begin{Bmatrix} \{\sigma\} \\ \{u\} \end{Bmatrix} = \begin{Bmatrix} 0 \\ -[F] \end{Bmatrix}. \quad (7)$$

The first matrix equation in (7) is the strain compatibility equations, which are written in stresses. The second matrix equation is the equilibrium equations of nodes. The matrix is block-diagonal form for any approximation variant from Table 1 and is easily reversible. Therefore, the system of equations (7) is conveniently solved in the following sequence:

$$[K] = [L][D]^{-1}[L]^T, \quad (8)$$

$$[K]\{u\} = \{F\}, \quad (9)$$

$$\{\sigma\} = [D]^{-1}[L]^T \{u\}. \quad (10)$$

Thus, solving the algebraic equations system (9), we obtain the nodal displacements values  $\{u\}$ , and then we shall calculate the stresses parameters vector  $\{\sigma\}$  from (10).

Next, we shall obtain the necessary expressions for  $[D]$ ,  $[L]$ ,  $[F]$ . For this we shall use variants stresses approximations, which are presented in Table 1.

### 2.1. Variant of approximation of stresses 1.

Let us introduce the notation for the unknown parameters vector of the finite element  $k$   $\{\sigma_k\}^T = (a_1 \ a_2 \ a_3 \ a_4 \ a_5 \ a_6 \ a_7)$  and for the stress approximations matrix

$$[H] = \begin{bmatrix} 1 & 0 & 0 & y & 0 & x & 0 \\ 0 & 1 & 0 & 0 & x & 0 & y \\ 0 & 0 & 1 & 0 & 0 & -y & -x \end{bmatrix}. \quad (11)$$

Then, the stresses vector of finite element  $k$

$$\{\sigma\} = \begin{Bmatrix} \sigma_x \\ \sigma_y \\ \tau_{xy} \end{Bmatrix} = [H]\{\sigma_k\} \quad (12)$$

Material stiffness matrix

$$[E]^{-1} = \frac{t}{E} \begin{bmatrix} 1 & -\mu & 0 \\ -\mu & 1 & 0 \\ 0 & 0 & 2(1+\mu) \end{bmatrix}. \quad (13)$$

$E$  is the material elasticity modulus;

$t$  is the plate thickness;

$\mu$  is the Poisson's coefficient.

The finite element flexibility matrix is defined by the following expression:

$$[D^k] = \iint [H]^T [E]^{-1} [H] d\Omega. \quad (14)$$

To obtain the solution and calculate the integral (14), we shall use the well-known transformation of the arbitrary quadrilateral element (Figure 1a) to the square element (Figure 1b). Such coordinate transformation can be written in the following form:

$$x = \sum_{i=1}^4 N_i(\xi, \eta) \cdot x_{i,k}, \quad y = \sum_{i=1}^4 N_i(\xi, \eta) \cdot y_{i,k}, \quad N_i(\xi, \eta) = \frac{1}{4}(1 + \xi_i \xi)(1 + \eta_i \eta). \quad (15)$$

$x_{i,k}$ ,  $y_{i,k}$  are the finite element nodes coordinates in the global coordinate system. The functions  $N_i(\xi, \eta)$  will later be used to specify the possible displacements over the finite element region (Figure 2). Therefore it is necessary to calculate the derivatives  $N_i(\xi, \eta)$  with respect to the coordinates  $x$  and  $y$ .

For partial derivatives of the function  $N_i(\xi, \eta)$  the following expressions can be written:

$$\frac{\partial N_i}{\partial \xi} = \frac{\partial N_i}{\partial x} \frac{\partial x}{\partial \xi} + \frac{\partial N_i}{\partial y} \frac{\partial y}{\partial \xi}, \quad \frac{\partial N_i}{\partial \eta} = \frac{\partial N_i}{\partial x} \frac{\partial x}{\partial \eta} + \frac{\partial N_i}{\partial y} \frac{\partial y}{\partial \eta}. \quad (16)$$

Index  $i$  denotes the local number node of the finite element (Figure 1a). The equations (16) may be written in the following matrix form:

$$\begin{Bmatrix} \frac{\partial N_i}{\partial \xi} \\ \frac{\partial N_i}{\partial \eta} \end{Bmatrix} = \begin{bmatrix} \frac{\partial x}{\partial \xi} & \frac{\partial y}{\partial \xi} \\ \frac{\partial x}{\partial \eta} & \frac{\partial y}{\partial \eta} \end{bmatrix} \begin{Bmatrix} \frac{\partial N_i}{\partial x} \\ \frac{\partial N_i}{\partial y} \end{Bmatrix}, \quad [J] = \begin{bmatrix} \frac{\partial x}{\partial \xi} & \frac{\partial y}{\partial \xi} \\ \frac{\partial x}{\partial \eta} & \frac{\partial y}{\partial \eta} \end{bmatrix}. \quad (17)$$

Using relations (15), we shall obtain the expressions of the matrix  $[J]$  elements:

$$\begin{aligned} J_{11} &= \frac{\partial x}{\partial \xi} = \sum_{i=1}^4 \frac{\xi_i(1+\eta\eta_i)}{4} x_{i,k} = \frac{1}{4} [(1-\eta)(x_{2,k} - x_{1,k}) + (1+\eta)(x_{3,k} - x_{4,k})], \\ J_{12} &= \frac{\partial y}{\partial \xi} = \sum_{i=1}^4 \frac{\xi_i(1+\eta\eta_i)}{4} y_{i,k} = \frac{1}{4} [(1-\eta)(y_{2,k} - y_{1,k}) + (1+\eta)(y_{3,k} - y_{4,k})], \\ J_{21} &= \frac{\partial x}{\partial \eta} = \sum_{i=1}^4 \frac{\eta_i(1+\xi\xi_i)}{4} x_{i,k} = \frac{1}{4} [(1-\xi)(x_{4,k} - x_{1,k}) + (1+\xi)(x_{3,k} - x_{2,k})], \\ J_{22} &= \frac{\partial y}{\partial \eta} = \sum_{i=1}^4 \frac{\eta_i(1+\xi\xi_i)}{4} y_{i,k} = \frac{1}{4} [(1-\xi)(y_{4,k} - y_{1,k}) + (1+\xi)(y_{3,k} - y_{2,k})]. \end{aligned} \quad (18)$$

From relation (17), we obtain the expressions of the necessary derivatives:

$$\begin{Bmatrix} \frac{\partial N_i}{\partial x} \\ \frac{\partial N_i}{\partial y} \end{Bmatrix} = [J]^{-1} \begin{Bmatrix} \frac{\partial N_i}{\partial \xi} \\ \frac{\partial N_i}{\partial \eta} \end{Bmatrix}, \quad [J]^{-1} = \begin{bmatrix} b_{11} & b_{12} \\ b_{21} & b_{22} \end{bmatrix}. \quad (19)$$

Matrix elements have the following expressions:

$$\det J = J_{11}J_{22} - J_{12}J_{21}, \quad b_{11} = \frac{J_{22}}{\det J}, \quad b_{12} = \frac{-J_{12}}{\det J}, \quad b_{21} = \frac{-J_{21}}{\det J}, \quad b_{22} = \frac{J_{11}}{\det J}. \quad (20)$$

Using the expression (19) and (15), we get

$$\begin{aligned} \frac{\partial N_i}{\partial x} &= b_{11} \frac{\xi_i(1+\eta\eta_i)}{4} + b_{12} \frac{\eta_i(1+\xi\xi_i)}{4}, \\ \frac{\partial N_i}{\partial y} &= b_{21} \frac{\xi_i(1+\eta\eta_i)}{4} + b_{22} \frac{\eta_i(1+\xi\xi_i)}{4}. \end{aligned} \quad (21)$$

Using the introduced coordinate transformation, the integral (14) can be written as follows:

$$[D^k] = \iint [H]^T [E]^{-1} [H] d\Omega = \int_{-1}^1 \int_{-1}^1 [H]^T [E]^{-1} [H] \cdot \det J d\eta d\xi. \quad (22)$$

To determine the matrix (22) elements, it is convenient to precompute the following integrals:

$$\begin{aligned} i_1 &= \int_{-1}^1 \int_{-1}^1 \det J d\eta d\xi = A, & i_2 &= \int_{-1}^1 \int_{-1}^1 x \cdot \det J d\eta d\xi, \\ i_3 &= \int_{-1}^1 \int_{-1}^1 y \cdot \det J d\eta d\xi, & i_4 &= \int_{-1}^1 \int_{-1}^1 x^2 \cdot \det J d\eta d\xi, \\ i_5 &= \int_{-1}^1 \int_{-1}^1 xy \cdot \det J d\eta d\xi, & i_6 &= \int_{-1}^1 \int_{-1}^1 y^2 \cdot \det J d\eta d\xi. \end{aligned} \quad (23)$$

Integrals (23) are calculated numerically using the four-point Gauss' formula. The following integration points and weight coefficients were taken in the calculations:

$$\begin{aligned} \xi_{g,1} = \eta_{g,1} &= \pm 0.339981, & W_1 &= 0.652145, \\ \xi_{g,2} = \eta_{g,2} &= \pm 0.861136, & W_2 &= 0.347855. \end{aligned} \quad (24)$$

Using expressions (22) and (23), we get:

$$[D^k] = \frac{t}{E} \begin{bmatrix} A & -\mu \cdot A & 0 & i_3 & -\mu \cdot i_2 & i_2 & -\mu \cdot i_3 \\ & A & 0 & -\mu \cdot i_3 & i_2 & -\mu \cdot i_2 & i_3 \\ & & 2(1+\mu)A & 0 & 0 & -2(1+\mu) \cdot i_3 & -2(1+\mu) \cdot i_2 \\ & & & i_6 & -\mu \cdot i_5 & i_5 & -\mu \cdot i_6 \\ & & & & i_4 & -\mu \cdot i_4 & i_5 \\ & & & & & i_4 + 2(1+\mu) \cdot i_6 & (2+\mu) \cdot i_5 \\ & & & & & & i_6 + 2(1+\mu) \cdot i_4 \end{bmatrix}. \quad (25)$$

*symmetrically*

The global flexibility matrix for the entire system  $[D]$  is formed from matrices flexibility  $[D^k]$  of finite elements.

To calculate matrix  $[L]$  elements we use the possible node displacement  $\delta u_i$  of the finite element (Figure 2) along the  $X$  axis:

$$\delta u_i = N_i(\xi, \eta) = \frac{1}{4}(1 + \xi_i \xi) \cdot (1 + \eta_i \eta). \quad (26)$$

Possible deformations that occur in the finite element are determined using expressions (21).

$$\begin{aligned}\delta\varepsilon_x &= \frac{\partial N_i}{\partial x} = b_{11} \frac{\xi_i(1+\eta\eta_i)}{4} + b_{12} \frac{\eta_i(1+\xi\xi_i)}{4}, \\ \delta\gamma_{xy} &= \frac{\partial N_i}{\partial y} = b_{21} \frac{\xi_i(1+\eta\eta_i)}{4} + b_{22} \frac{\eta_i(1+\xi\xi_i)}{4}.\end{aligned}\quad (27)$$

We introduce the notation of the possible deformations vector of the finite element  $k$

$$\{\delta\varepsilon_k\} = \begin{Bmatrix} \delta\varepsilon_x \\ \delta\varepsilon_y \\ \delta\gamma_{xy} \end{Bmatrix} = \begin{Bmatrix} b_{11} \frac{\xi_i(1+\eta\eta_i)}{4} + b_{12} \frac{\eta_i(1+\xi\xi_i)}{4} \\ 0 \\ b_{21} \frac{\xi_i(1+\eta\eta_i)}{4} + b_{22} \frac{\eta_i(1+\xi\xi_i)}{4} \end{Bmatrix}.\quad (28)$$

The work of internal forces is

$$\delta U_{i,x}^k = t \iint_{\Omega_k} \{\delta\varepsilon_k\} \{\sigma\}^T d\Omega = t \int_{-1}^1 \int_{-1}^{-1} \{\delta\varepsilon_k\}^T [H] \{\sigma_k\} \det J d\eta d\xi = \{C_{i,x}^k\}^T \{\sigma_k\}.\quad (29)$$

In (29) the notation is entered:

$$\{C_{i,x}^k\}^T = t \int_{-1}^1 \int_{-1}^{-1} \{\delta\varepsilon_k\}^T [H] \det J d\eta d\xi.\quad (30)$$

To calculate the vector  $\{C_{i,x}^k\}$  elements it is convenient to pre-compute numerically. For that we use the four-point Gauss' formula, the following integrals:

$$\begin{aligned}\alpha_{1,i} &= t \int_{-1}^1 \int_{-1}^{-1} \frac{\partial N_i}{\partial x} \det J d\eta d\xi, & \alpha_{1,x,i} &= t \int_{-1}^1 \int_{-1}^{-1} \frac{\partial N_i}{\partial x} x \cdot \det J d\eta d\xi, & \alpha_{1,y,i} &= t \int_{-1}^1 \int_{-1}^{-1} \frac{\partial N_i}{\partial x} y \cdot \det J d\eta d\xi, \\ \alpha_{2,i} &= t \int_{-1}^1 \int_{-1}^{-1} \frac{\partial N_i}{\partial y} \det J d\eta d\xi, & \alpha_{1,y,i} &= t \int_{-1}^1 \int_{-1}^{-1} \frac{\partial N_i}{\partial y} x \cdot \det J d\eta d\xi, & \alpha_{2,y,i} &= t \int_{-1}^1 \int_{-1}^{-1} \frac{\partial N_i}{\partial y} y \cdot \det J d\eta d\xi.\end{aligned}\quad (31)$$

Using (11), (28), (30) and (31) we get

$$\{C_{i,x}^k\}^T = (\alpha_{1,i} \quad 0 \quad \alpha_{2,i} \quad \alpha_{1,y,i} \quad 0 \quad (\alpha_{1,x,i} - \alpha_{2,y,i}) \quad -\alpha_{2,x,i}).\quad (32)$$

Next, we consider the possible displacement of finite element node along the  $Y$  axis

$$\delta v_i = N_i(\xi, \eta) = \frac{1}{4}(1 + \xi_i \xi)(1 + \eta_i \eta).\quad (33)$$

The possible deformations that occur in the finite element are determined using expressions (21).

$$\begin{aligned}\delta\varepsilon_y &= \frac{\partial N_i}{\partial y} = b_{21} \frac{\xi_i(1+\eta\eta_i)}{4} + b_{22} \frac{\eta_i(1+\xi\xi_i)}{4}, \\ \delta\gamma_{xy} &= \frac{\partial N_i}{\partial x} = b_{11} \frac{\xi_i(1+\eta\eta_i)}{4} + b_{12} \frac{\eta_i(1+\xi\xi_i)}{4}.\end{aligned}\quad (34)$$

Performing similar transformations, which are given above, we shall get:

$$\delta U_{i,y}^k = \{C_{i,y}^k\}^T \{\sigma_k\},\quad (35)$$

$$\{C_{i,y}^k\}^T = (0 \quad \alpha_{2,i} \quad \alpha_{1,i} \quad 0 \quad \alpha_{2,x,i} \quad -\alpha_{1,y,i} \quad (-\alpha_{1,x,i} + \alpha_{2,y,i})).\quad (36)$$

We combine the internal force works at the possible displacements for all finite element nodes into the vector

$$\{\delta U^k\}^T = (\delta U_{1,x}^k \quad \delta U_{1,y}^k \quad \delta U_{2,x}^k \quad \delta U_{2,y}^k \quad \delta U_{3,x}^k \quad \delta U_{2,y}^k \quad \delta U_{4,x}^k \quad \delta U_{4,y}^k). \quad (37)$$

Rows (32) and (36) are combined into the matrix

$$[L^k] = \begin{bmatrix} \alpha_{1,1} & 0 & \alpha_{2,1} & \alpha_{1,y,1} & 0 & (\alpha_{1,x,1} - \alpha_{2,y,1}) & -\alpha_{2,x,1} \\ 0 & \alpha_{2,1} & \alpha_{1,1} & 0 & \alpha_{2,x,1} & -\alpha_{1,y,1} & (-\alpha_{1,x,1} + \alpha_{2,y,1}) \\ \alpha_{1,2} & 0 & \alpha_{2,2} & \alpha_{1,y,2} & 0 & (\alpha_{1,x,2} - \alpha_{2,y,2}) & -\alpha_{2,x,2} \\ 0 & \alpha_{2,2} & \alpha_{1,2} & 0 & \alpha_{2,x,2} & -\alpha_{1,y,2} & (-\alpha_{1,x,2} + \alpha_{2,y,2}) \\ \alpha_{1,3} & 0 & \alpha_{2,3} & \alpha_{1,y,3} & 0 & (\alpha_{1,x,3} - \alpha_{2,y,3}) & -\alpha_{2,x,3} \\ 0 & \alpha_{2,3} & \alpha_{1,3} & 0 & \alpha_{2,x,3} & -\alpha_{1,y,3} & (-\alpha_{1,x,3} + \alpha_{2,y,3}) \\ \alpha_{1,4} & 0 & \alpha_{2,4} & \alpha_{1,y,4} & 0 & (\alpha_{1,x,4} - \alpha_{2,y,4}) & -\alpha_{2,x,4} \\ 0 & \alpha_{2,4} & \alpha_{1,4} & 0 & \alpha_{2,x,4} & -\alpha_{1,y,4} & (-\alpha_{1,x,4} + \alpha_{2,y,4}) \end{bmatrix}. \quad (38)$$

Using (37) and (38) we can write

$$\{\delta U^k\} = [L^k] \{\sigma^k\}. \quad (39)$$

The matrix  $[L]$  is formed from the finite element matrices  $[L^k]$ .

Since unknown stresses parameters  $\{\sigma_k\}^T = (a_1 \ a_2 \ a_3 \ a_4 \ a_5 \ a_6 \ a_7)$  are independent for finite elements, the formation of the resolving equations system can be performed in the same way as it is done for the finite element method in displacements. In this case, for each finite element we can form the matrix

$$[B^k] = [L^k][D^k][L^k]^T. \quad (40)$$

Then, from the matrices  $[B^k]$ , in accordance with the node numbering, the matrix  $[K]$  is formed for the equations system (9). The matrix  $[B^k]$  is an analogue of the finite element stiffness matrix.

To form vector  $\{F\}$ , it is necessary to calculate the work of loads distributed over the finite element at possible node displacements:

$$\delta V_{i,x}^k = \int_{\Omega_k} q_x^k \delta u_i d\Omega = \int_{-1}^1 \int_{-1}^1 q_x^k N_i(\xi, \eta) \cdot \det J d\eta d\xi = P_{x,i}^k, \quad (41)$$

$$\delta V_{i,y}^k = \int_{\Omega_k} q_y^k \delta v_i d\Omega = \int_{-1}^1 \int_{-1}^1 q_y^k N_i(\xi, \eta) \cdot \det J d\eta d\xi = P_{y,i}^k. \quad (42)$$

To calculate (41), (42) for each finite element node ( $i = 1, 2, 3, 4$ ), the Gauss' numerical integration procedure is used. In accordance with the nodes numbering forces  $P_{x,i}^k$  and  $P_{y,i}^k$  are summed with the corresponding elements of the vector  $\{F\}$ . The concentrated in the nodes forces  $P_x, P_y$  are also added to the elements of the vector  $\{F\}$ .

## 2.2. Variants of approximation of stresses 2 and 3

All solving equations for these variants coincide with the equations for variant 1. It is necessary to simply exclude some columns of the matrices  $[L^k]$ , which is corresponding of the excluded parameters, and the same rows and columns of the matrices  $[D^k]$  (see Table 1).

## 2.3. Variant of approximation of stresses 4

As unknown parameters the stresses values in the nodes of the finite element grid  $\sigma_{x,i}, \sigma_{y,i}, \tau_{xy,i}$  are used directly. In this case the stresses are constant values in each of the finite element regions  $\Omega_1 \div \Omega_4$  and





The matrix  $[L^k]$  consists of lines (48):

$$[L^k] = \begin{bmatrix} \beta_{1,1}^x & 0 & \beta_{1,1}^y & \beta_{1,2}^x & 0 & \beta_{1,2}^y & \beta_{1,3}^x & 0 & \beta_{1,3}^y & \beta_{1,4}^x & 0 & \beta_{1,4}^y \\ 0 & \beta_{1,1}^y & \beta_{1,1}^x & 0 & \beta_{1,2}^y & \beta_{1,2}^x & 0 & \beta_{1,3}^y & \beta_{1,3}^x & 0 & \beta_{1,4}^y & \beta_{1,4}^x \\ \beta_{2,1}^x & 0 & \beta_{2,1}^y & \beta_{2,2}^x & 0 & \beta_{2,2}^y & \beta_{2,3}^x & 0 & \beta_{2,3}^y & \beta_{2,4}^x & 0 & \beta_{2,4}^y \\ 0 & \beta_{2,1}^y & \beta_{2,1}^x & 0 & \beta_{2,2}^y & \beta_{2,2}^x & 0 & \beta_{2,3}^y & \beta_{2,3}^x & 0 & \beta_{2,4}^y & \beta_{2,4}^x \\ \beta_{3,1}^x & 0 & \beta_{3,1}^y & \beta_{3,2}^x & 0 & \beta_{3,2}^y & \beta_{3,3}^x & 0 & \beta_{3,3}^y & \beta_{3,4}^x & 0 & \beta_{3,4}^y \\ 0 & \beta_{3,1}^y & \beta_{3,1}^x & 0 & \beta_{3,2}^y & \beta_{3,2}^x & 0 & \beta_{3,3}^y & \beta_{3,3}^x & 0 & \beta_{3,4}^y & \beta_{3,4}^x \\ \beta_{4,1}^x & 0 & \beta_{4,1}^y & \beta_{4,2}^x & 0 & \beta_{4,2}^y & \beta_{4,3}^x & 0 & \beta_{4,3}^y & \beta_{4,4}^x & 0 & \beta_{4,4}^y \\ 0 & \beta_{4,1}^y & \beta_{4,1}^x & 0 & \beta_{4,2}^y & \beta_{4,2}^x & 0 & \beta_{4,3}^y & \beta_{4,3}^x & 0 & \beta_{4,4}^y & \beta_{4,4}^x \end{bmatrix}. \quad (49)$$

The global  $[L]$  matrix is formed from the all finite elements matrices  $[L^k]$ . Note that in this case the direct matrix  $[K]$  formation, by calculating the matrix  $[B^k]$  (see (40)) for each finite element, is impossible. The expressions of the load's potential (41), (42) don't depend on the stresses approximations types.

Note that the width of the nonzero elements tape for the matrix  $[K]$  is approximately two times the tape width of the equations system for the finite element method in displacements and the matrix  $[K]$  tape width for variants of stresses approximations 1–3.

### 3. Results and Discussion

An analytical solution for ring loaded with concentrated forces is given in [23]. Due to symmetry, a quarter of the ring was calculated. That is shown in Figure 3a. The ring has an inner radius  $r$  and an outer radius  $R = 2 \cdot r$ . To solve the problem, the following ring parameters were taken:  $E = 10\,000 \text{ kN/m}^2$ ,  $\mu = 0.3$ ,  $r = 3 \text{ m}$ ,  $P = 20 \text{ kN}$ . In nodes are along the line  $AB$ , we excluded displacements which directed along the  $X$  axis, in nodes are along line  $CD$ , we excluded displacements which directed along the  $Y$  axis.

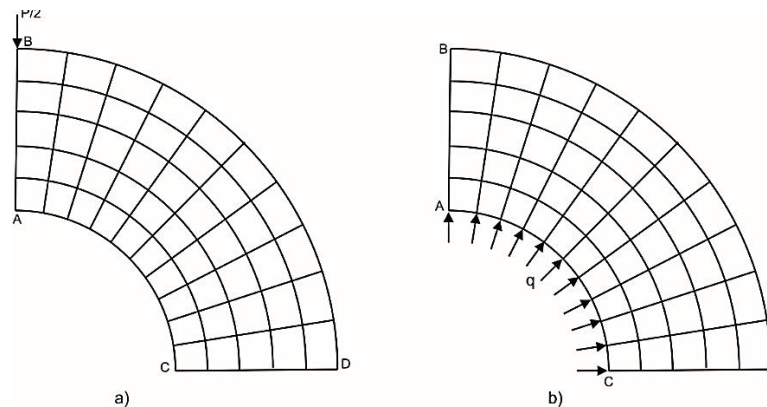


Figure 3. A quarter of the ring (the grid of 5x10 finite elements).  
a) concentrated force  $P$ ; b) uniform internal pressure  $q$ .

Table 3 shows the displacements values of point  $C$  for different finite element grids. The values in the Table 3 show the displacements convergence rapid. For the case piecewise constant approximation of stresses (variant 4), there is strict displacements convergence to the exact value from above.

Table 3. Displacement  $100u_c, \text{ m}$  (Figure 3a).

Grid	Variants of the stress approximations			
	1	2	3	4
5x10	0.60274	0.61341	0.62238	0.66561
10x20	0.61633	0.61902	0.62146	0.63407
20x40	0.61993	0.62061	0.62123	0.62461
30x60	0.62061	0.62091	0.62119	0.62272

In [23], the analytically calculate stresses values are given for nodes which lay at the lines  $AB$  and  $CD$  (Figure 3a). Stress values are given in dimensionless form:

$$\bar{\sigma}_{x(y)} = \frac{\pi R}{2P} \sigma_{x(y)}. \quad (50)$$

For the solutions comparison, the stresses values at the indicated points, which were obtained for the finite element mesh  $10 \times 20$ , are given in Tables 4 and 5. Stresses were calculated for four stress approximations variants. For approximations 1–3, the stresses are discontinuous along the element boundaries. Therefore, in Table 4 for the grid internal nodes, two values are given. These values were calculated in the two finite elements which are adjoining at the node. In each finite element, stresses were calculated for the corresponding node point. To do this, node coordinates were substituted into the stress expressions (Table 1). For the variant 4, the stresses are calculated directly for the grid nodes, therefore one value was presented.

**Table 4. Stresses  $\bar{\sigma}_y$  at nodes along the CD line.**

Node	Variant of approximations				Value of [23]
	1	2	3	4	
1-C	-8.833	-8.819	-7.690	-8.391	-8.942
2	-6.311	-6.210	-7.690	-6.412	-
	-6.342	-6.355	-5.518		
3	-4.561	-4.483	-5.518	-4.682	-4.610
	-4.519	-4.538	-3.892		
4	-3.183	-3.116	-3.892	-3.163	-
	-3.105	-3.121	-2.559		
5	-2.043	-1.980	-2.559	-2.052	-2.012
	-1.948	-1.958	-1.518		
6	-1.059	-0.998	-1.518	-0.999	-
	-0.956	-0.961	-0.574		
7	-0.179	-0.118	-0.574	-0.133	-0.113
	-0.073	-0.073	0.280		
8	0.632	0.694	0.280	0.715	-
	0.738	0.742	1.076		
9	1.396	1.459	1.076	1.478	1.477
	1.501	1.508	1.832		
10	2.129	2.192	1.832	2.233	-
	2.234	2.242	2.563		
11-D	2.842	2.903	2.563	2.798	2.940

**Table 5. Stresses  $\bar{\sigma}_x$  at nodes along the CD line.**

Node	Variant of approximations				Value of [23]
	1	2	3	4	
1-A	9.818	9.807	8.144	9.399	10.147
2	6.162	6.019	8.144	6.216	-
	6.050	6.075	5.086		
3	4.002	3.915	5.086	4.200	4.002
	3.778	3.797	3.173		
4	2.500	2.434	3.173	2.421	-
	2.231	2.234	1.804		
5	1.350	1.289	1.804	1.299	1.24
	1.055	1.037	0.749		
6	0.390	0.326	0.749	0.532	-
	0.065	0.020	-0.213		
7	-0.482	-0.567	-0.213	-0.546	-0.594
	-0.850	-0.949	-1.021		
8	-1.354	-1.452	-1.021	-0.433	-
	-1.785	-1.974	-1.971		
9	-2.423	-2.679	-1.971	-3.134	-2.185
	-2.893	-3.394	-3.370		
10	-4.164	-4.273	-3.370	-5.852	-
	-5.005	-5.757	-3.187		
11-B	-13.562	-15.832	-3.187	-19.300	-3.788

The results analysis, which is given in Tables 3–5, shows that less accurate stresses values were obtained for the third stress approximation variant. The stress values of the first and second variants are close, but the first variant gives closer stress values to the analytical solution at the extreme nodes. In intermediate nodes, the 1–3 approximation variants have discontinuities in the stresses, therefore, the deviations from the

analytical solution are more significant compared with the fourth variant. To improve the results accuracy for variants 1–3, it is necessary to calculate the average stresses values for intermediate grid nodes. The fourth variant of stresses approximations allows one to obtain stresses directly at the grid nodes and ensures the displacements convergence to exact values from above. It should be noted that point  $B$  is the point of singularity. At this node, the stresses tend to infinity, so it is impossible to compare values for this point. But it is obvious that the analytical solution [23] for this point does not provide the drastic change of the stress's values. Therefore, the value  $\bar{\sigma}_{x,B} = -3.788$  can't serve as the reference of comparison with other solutions.

In addition, the stress value  $\bar{\sigma}_{x,9} = -2.185$  in the neighboring node is also unreliable, that is due to the inaccuracy of the analytical solution in the singularity zone. Note that the solutions of the approximation's variants 1, 2 and 4 more accurately represent the stresses change at the singularity zone and allow us to obtain more accurate and consistent stress values.

When using the finite element method in displacements, usually, the stresses are determined not at the nodal points, but at the finite element centers. If we want to improve the accuracy of their values, the finite element grid should be grinding. Tables 6–8 show the stresses at the finite element centers, which is adjacent to points  $C$ ,  $D$  and  $A$ , for the considered stresses approximations variants, as well as those obtained using the LIRA-SAPR program. For variant 4, the stress values are given directly for the nodes.

**Table 6. Stress  $\bar{\sigma}_y$  at the finite element closest to point  $C$ . Analytical value  $\bar{\sigma}_y = -8.942$ .**

Grid	Variant of approximations				LIRA-SAPR
	1	2	3	4	
5x10	-6.431	-8.437	-6.629	-8.078	-6.120
10x20	-7.559	-8.819	-7.628	-8.391	-7.449
20x40	-8.199	-8.908	-8.219	-8.618	-8.167
30x60	-8.425	-8.917	-8.434	-8.698	-8.411

**Table 7. Stress  $\bar{\sigma}_y$  at the finite element closest to point  $D$ . Analytical value  $\bar{\sigma}_y = 2.940$ .**

Grid	Variant of approximations				LIRA-SAPR
	1	2	3	4	
5x10	2.129	2.869	2.267	2.734	2.146
10x20	2.549	2.903	2.589	2.798	2.547
20x40	2.745	2.917	2.755	2.826	2.744
30x60	2.807	2.921	2.812	2.888	2.807

**Table 8. Stress  $\bar{\sigma}_x$  in the finite element closest to point  $A$ . Analytical value  $\bar{\sigma}_x = 10.147$ .**

Grid	Variant of approximations				LIRA-SAPR
	1	2	3	4	
5x10	6.301	6.359	6.501	8.977	5.850
10x20	7.967	7.975	8.098	9.399	7.811
20x40	8.980	8.980	9.007	9.679	8.931
30x60	9.352	9.351	9.365	9.803	9.329

The values given in Tables 6–8 show that approximation variants 2 and 4 provide the greatest accuracy. At the smallest grid, for point  $A$  by 5 % more accurate stresses values are calculated by the fourth version of approximations, and for points  $C$  and  $D$  by 2–3 % the second variant is more accurate. The stresses values obtained by the LIRA-SAPR program are less accurate compared to variants 2 and 4, by about 5–6 %, and their values are smaller.

The analytical solution for ring loaded with uniform internal pressure (Figure 3b) is given in [15]. For the CD line, this solution can be written as follows:

$$\sigma_x = \frac{qr^2}{R^2 - r^2} \left( 1 - \frac{R^2}{x^2} \right), \sigma_y = \frac{qr^2}{R^2 - r^2} \left( 1 + \frac{R^2}{x^2} \right), \tau_{xy} = 0, u = \frac{qr^2 x (1 + \mu)}{E (R^2 - r^2)} \left( 1 - 2\mu + \frac{R^2}{x^2} \right). \quad (51)$$

To estimate the proposed method accuracy, quarter-ring calculations were performed (Figure 3b) with different finite element meshes for the stress approximation variants 1–4, as well as using the LIRA-SAPR program. The following ring parameters were used for calculations:  $E = 10\,000$  kN/m<sup>2</sup>,  $\mu = 0.3$ ,  $r = 3$  m,  $q = 10$  kN/m.

**Table 9. Displacement  $100u_c$ , m (Figure 3b).**

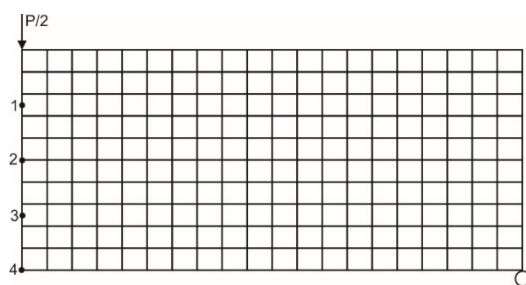
Grid	Variant of approximations				LIRA-SAPR
	1	2	3	4	
5×10	0.5893	0.5925	0.5891	0.5943	0.5859
10×20	0.5898	0.5907	0.5897	0.5913	0.5890
20×40	0.5900	0.5902	0.5899	0.5903	0.5897
30×60	0.5900	0.5901	0.5900	0.5902	0.5900
Exact value 0.5720					

The displacements of point  $C$  for the four stresses approximation variants are given in Table 9. All variants show good accuracy and fast convergence of the displacement value. With the grid of 30×60, the solutions practically coincide for all the considered variants. Variants 2 and 4 demonstrate convergence to the exact value from above.

**Table 10. Stresses at points  $C$  and  $B$  (Figure 3b) for various approximation variants.**

Grid	Variant	$\sigma_{x,C}$ , kN/m <sup>2</sup>		$\sigma_{y,C}$ , kN/m <sup>2</sup>		$\sigma_{y,B}$ , kN/m <sup>2</sup>	
		node	f. e.	node	f. e.	node	f. e.
5×10	1	-8.040	-7.598	16.919	14.383	6.580	7.004
10×20		-8.961	-8.737	16.887	15.440	6.629	6.834
20×40		-9.463	-9.352	16.804	16.028	6.650	6.750
30×60		<b>-9.637</b>	<b>-9.354</b>	<b>16.765</b>	<b>16.235</b>	<b>6.656</b>	<b>6.722</b>
5×10	2	-7.808	-7.668	16.572	14.252	6.559	7.091
10×20		-8.794	-8.754	16.819	15.391	6.616	6.859
20×40		-9.366	-9.355	16.802	16.013	6.642	6.757
30×60		<b>-9.570</b>	<b>-9.565</b>	<b>16.771</b>	<b>16.228</b>	<b>6.650</b>	<b>6.725</b>
5×10	3	-8.233	-7.605	14.739	14.480	7.030	6.948
10×20		-9.102	-8.743	15.546	15.478	6.837	6.818
20×40		-9.546	-9.354	16.058	16.040	6.750	6.746
30×60		<b>-9.698</b>	<b>-9.565</b>	<b>16.233</b>	<b>16.241</b>	<b>6.722</b>	<b>6.720</b>
5×10	4	-9.427		15.874		6.891	
10×20		-9.875		16.079		6.807	
20×40		-9.967		16.318		6.728	
30×60		<b>-9.985</b>		<b>16.420</b>		<b>6.706</b>	
5×10	LIRA-SAPR		-7.595		14.013		6.934
10×20			-8.739		15.325		6.817
20×40			-9.352		15.996		6.746
30×60			<b>-9.569</b>		<b>16.224</b>		<b>6.722</b>
Exact value			<b>-10</b>		<b>16.6667</b>		<b>6.6667</b>

The stresses at points  $B$  and  $C$  for different finite element meshes are given in Table 10. The stresses for approximations 1–3 were determined twice. The first value (title column is “f. e.”) is the stresses at the center of the finite element, which is adjacent to the corresponding point. The second value (title column is “node”) is the stresses were determined by substituting the node coordinates into the expression for the stress approximation functions (see Table 1). Comparison of the obtained results with exact values shows that the fourth variant has the best accuracy. The remaining variants have similar stresses values. With the greatest error, approximately 2.7 %, the stress values were calculated of third approximation variant and according to the LIRA-SCAD program. Of course, the stress values calculated for the nodes are more accurate.

**Figure 4. Half of hinged supported beam. Finite element grid 10×20.**

Also, calculations were carried out of hinged supported beam on the concentrated force action. Figure 4 shows half of the beam. The following parameters were adopted: span is 4 m, section height is  $h = 1$  m, section width is  $b = 1.0$  m,  $E = 10\,000$  kN/m<sup>2</sup>,  $\mu = 0.3$ ,  $P = 10$  kN. The book [23] provides analytical solutions for stresses in sections which is located near the concentrated force application point. The stresses values are presented in the following form:

$$\sigma_x = \sigma_{x,b} + \beta_x \left( \frac{2P}{h} \right), \sigma_y = \beta_y \left( \frac{2P}{h} \right). \tag{52}$$

$\sigma_{x,b}$  is the stress which was calculated by the beam theory in accordance with the Kirchhoff's hypothesis. The stresses values calculated in accordance with (52) for points 1–4 are given in Table 11.

**Table 11. Analytical solution for the beam [23].**

Point	$\beta_x$	$\sigma_x$ , kN/m <sup>2</sup>	$\beta_y$	$\sigma_y$ , kN/m <sup>2</sup>
1	0.428	-20.44	-1.230	-24.6
2	0.121	2.42	-0.456	-9.12
3	-0.136	27.28	-0.145	-2.90
4	-0.133	57.32	0	0

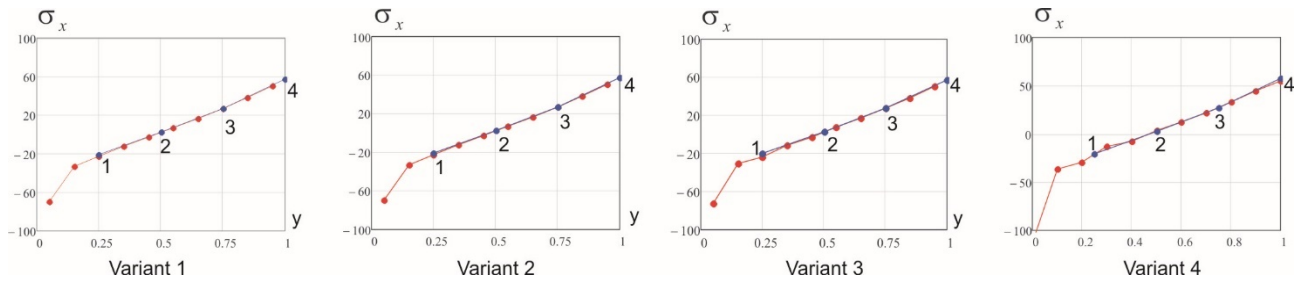


**Figure 5. Stresses  $\sigma_x$  at the finite element centers, which lay on line 1–4, in the beam middle section (Figure 4). The blue line is the analytical solution.**

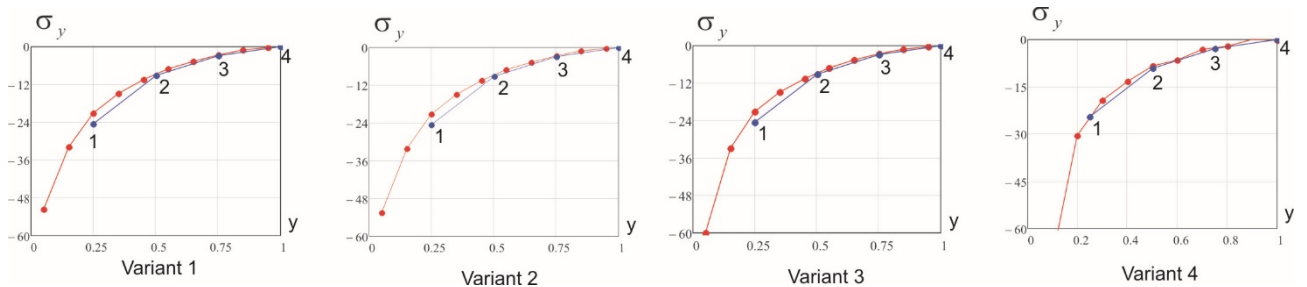


**Figure 6. Stresses  $\sigma_y$  at the finite element centers, which lay on line 1–4, in the beam middle section (Figure 4). The blue line is the analytical solution.**

The Figures 5–6 present the solutions for the considered stresses approximations variants, when was using the rather coarse 10×20 grid. The obtained solutions are in good agreement with the analytical solution. The fourth stresses approximations variant which use the piecewise constant functions allows to obtain the most accurate solutions for stresses. For variants 1–3, the greatest difference from the analytical solution is observed at point 1 which is closest to the point of concentrated force application and is the singularity point. Table 12 shows the obtained by the proposed methods stresses values.

**Table 12. Stresses at point 1 (Figures 5–6).**

Stress	Variant of approximations			Exact value
	1	2	3	
$\sigma_x$ , kN/m <sup>2</sup>	-22.58	-22.67	-23.91	-20.44
$\sigma_y$ , kN/m <sup>2</sup>	-21.09	-21.10	-21.03	-24.60

As in the previous examples, the approximation variants 1 and 2 provide closer to exact stresses values (Table 12). The stresses  $\sigma_x$  differ from the exact ones by about 11 %, and the stresses  $\sigma_y$  – by 14 %. Note that the solution of variant 4 practically coincides with the analytical solution at all points which lay along the height of the section.

In [1], algorithm the stiffness matrix constructing of rectangular finite element, which was based on the second stresses approximations variant, is considered. To build the stiffness matrix at first the strains are expressed through the stresses. Then the displacement functions are determined by integrating the deformations expressions. As a result, the displacements expressions turn out to be dependent on the transverse deformations coefficient. It is noted that for such element the inter-element displacements continuity is not provided. On the example of the cantilever beam calculation, it is shown that this element provides fast displacements convergence to the exact solution.

The approach proposed in this paper allows us to develop various equilibrium finite elements which are based on the fundamental principles of the additional energy minimum and possible displacements. These elements can be used for plane theory elasticity problems. The proposed method is based on stresses fields approximations. The considered stresses approximations variants showed good accuracy and convergence for test problems, when we grind the finite element grid. The best accuracy is demonstrated by stresses approximations variants 4, 1 and 2.

## 4. Conclusion

1. The method is proposed for constructing equilibrium arbitrary quadrangular finite elements for solving plane problems in the elasticity theory. The technique is based on the principles of additional energy minimum and possible displacements and it provides to use the necessary approximations of stresses.

2. Comparison of the solutions which were obtained by the proposed method with analytical solutions for the ring and the bent beam is performed. The best accuracy is provided by the variant which use piecewise constant approximations of stresses over finite element region. The deviation calculated values from exact solutions does not exceed 2 %. Such stresses approximations can provide the displacements convergence to exact values from above.

3. The stresses approximations which are based on variants 1 and 2 are discontinuous along the finite elements' boundaries, but also provide good accuracy in the stress' determination. Even we use coarse grids, the deviation calculated values from the exact solutions is 5–6 %. Such finite elements can be convenient when we must solve branched and combined structures.

4. The proposed method can be further used to build equilibrium triangular finite elements and to solve bulk problems of the elasticity theory.

## References

- Zenkevich, O. Metod konechnykh elementov v tekhnike [The finite element method in technique]. Moscow: Mir, 1975. 541 p. (rus)
- Zenkevich, O., Morgan, K. Konechnyye elementy i approksimatsiya [Finite Elements and Approximations]. Moscow: Mir, 1986. 318 p. (rus)
- Gallager, R. Metod konechnykh elementov. Osnovy [Finite element method. The basics]. Moscow: Mir, 1984. 428 p. (rus)
- Artioli, E., de Miranda, S., Lovadina, C., Patruno, L. A stress/displacement Virtual Element method for plane elasticity problems. *Comput. Methods Appl. Mech. Eng.* 2017. Vol. 325. Pp. 155–174.
- Chernysheva, N.V., Kolosova, G.S., Rozin, L.A. Combined method of 3d analysis for underground structures in view of surrounding infinite homogeneous and inhomogeneous medium. *Magazine of Civil Engineering.* 2016. No. 2 (62). Pp. 83–91. DOI: 10.5862/MCE.62.8
- Tyukalov, Yu.Ya. Refined finite element of rods for stability calculation. *Magazine of Civil Engineering.* 2018. 79(3). Pp. 54–65. DOI: 10.18720/MCE.79.6
- Lalin, V.V., Rozin, L.A., Kushova, D.A. Variatsionnaya postanovka ploskoy zadachi geometricheski nelineynogo deformirovaniya i ustoychivosti uprugikh sterzhney [Variational statement of a plane problem geometrically nonlinear deformation and stability elastic rods]. *Magazine of Civil Engineering.* 2013. 36(1). Pp. 87–96. (rus) DOI: 10.5862/MCE.36.11.
- Artioli, E., Miranda, S., Lovadina, C., Patruno, L. A family of virtual element methods for plane elasticity problems based on the Hellinger–Reissner principle. *Computer Methods in Applied Mechanics and Engineering.* 2018. 340. Pp. 978–999.
- Li, Z., Chen, S., Qu, S., Li, M. Stabilization of low-order mixed finite elements for the plane elasticity equations // *Computers & Mathematics with Applications.* 2017. 73. Pp. 363–373.
- Leonetti, L., Garcea, G., Nguyen-Xuan, H. A mixed edge-based smoothed finite element method (MES-FEM) for elasticity. *Computers & Structures.* 2016. Vol. 173. Pp. 123–138.
- Elakkad, A., Bennani, M.A., Mekkaoui, J., Elkhalfi, A.A. Mixed Finite Element Method for Elasticity Problem. *International Journal of Advanced Computer Science and Applications.* 2013. Vol. 4. No. 2. Pp. 161–166.
- Mirsaidov, M.M., Abdikarimov, R.A., Vatin, N.I., Zhgutov, V.M., Khodzhayev, D.A., Normuminov, B.A. Nonlinear parametric oscillations of viscoelastic plate of variable thickness. *Magazine of Civil Engineering.* 2018. 82(6). Pp. 112–126. DOI: 10.18720/MCE.82.11
- Sukhoterlin, M.V., Baryshnikov, S.O., Knysh, T.P., Abdikarimov, R.A. Natural oscillations of a rectangular plates with two adjacent edges clamped. *Magazine of Civil Engineering.* 2018. No. 6(82). Pp. 81–94. DOI: 10.18720/MCE.82.8.
- Wang, Q., Zhou, W., Cheng, Y., Ma, G., Chang, X., Chen, E. NE-IIBEFM for problems with body forces: a seamless integration of the boundary type meshfree method and the NURBS boundary in CAD. *Adv. Eng. Softw.* 2018. Vol. 11. Pp. 1–17.
- Zhou, W., Yue, Q., Wang, Q., Feng, Y.T., Chang, X. The boundary element method for elasticity problems with concentrated loads based on displacement singular elements. *Engineering Analysis with Boundary Elements.* 2019. Vol. 99. Pp. 195–205.
- Gu, Y., Zhang, C., Qu, W., Ding, J. Investigation on near-boundary solutions for three-dimensional elasticity problems by an advanced BEM. *Int. J. Mech. Sci.* 2018. Vol. 142. Pp. 269–275.

17. Zhou, J., Wang, K., Li, P. A hybrid fundamental-solution-based 8-node element for axisymmetric elasticity problems. *Engineering Analysis with Boundary Elements*. 2019. Vol. 101. Pp. 297–309.
18. Lin, Mu, Junping, Wang, Xie, Ye. A hybridized formulation for the weak Galerkin mixed finite element method. *Journal of Computational and Applied Mathematics*. 2016. Vol. 307. Pp. 335–345.
19. Tyukalov, Yu.Ya. Finite element models in stresses for bending plates. *Magazine of Civil Engineering*. 2018. 82(6). Pp. 170–190. DOI: 10.18720/MCE.82.16
20. Tyukalov, Yu.Ya. Finite element models in stresses for plane elasticity problems. *Magazine of Civil Engineering*. 2018. 77(1). Pp. 23–37. DOI: 10.18720/MCE.77.3.
21. Tyukalov, Yu.Ya. Finite element model of Reisner's plates in stresses. *Magazine of Civil Engineering*. 2019. 89(5). Pp. 61–78. DOI: 10.18720/MCE.89.6
22. Tyukalov, Yu.Ya. Calculation method of bending plates with assuming shear deformations. *Magazine of Civil Engineering*. 2019. 85(1). Pp. 107–122. DOI: 10.18720/MCE.85.9.
23. Timoshenko, S.P., Gudyer, Dzh. *Teoriya uprugosti [Elasticity theory]*. Moskow: Nauka, 1979. 560 p. (rus)

**Contacts:**

*Yury Tyukalov, +7(912)8218977; yutvgu@mail.ru*

© Tyukalov, Yu.Ya., 2019





DOI: 10.18720/MCE.91.8

## Равновесные конечные элементы для плоских задач теории упругости

Ю.Я. Тюкалов

Вятский государственный университет, г. Киров, Россия

\* E-mail: [yutvgu@mail.ru](mailto:yutvgu@mail.ru)

**Ключевые слова:** аппроксимации напряжений, дополнительная энергия, метод конечных элементов, плоская задача

**Аннотация.** Работа посвящена построению конечных элементов на основе аппроксимации напряжений для решения плоских задач теории упругости. Такие элементы являются альтернативными существующим конечным элементам, полученным с использованием аппроксимации перемещений. Альтернативные решения позволяют более точно оценивать напряженно-деформированное состояние конструкции. Предлагаемая методика построения конечных элементов основывается на принципах минимума дополнительной энергии и возможных перемещений. Рассматриваются различные варианты аппроксимации напряжений, которые удовлетворяют дифференциальным уравнениям равновесия для случая отсутствия распределенной нагрузки. Выполнено сравнение решений, полученных по предлагаемой методике, с аналитическими решениями для кольца и изгибаемой балки. Рассмотренные варианты аппроксимации напряжений показывают для тестовых задач хорошую точность и сходимость при измельчении сетки конечных элементов. Показано, что лучшую точность вычисления напряжений и перемещений обеспечивает конечный элемент с кусочно-постоянными аппроксимациями напряжений. Кроме того, такой конечный элемент обеспечивает сходимость перемещений к точным значениям сверху. Другие варианты конечных элементов могут быть удобны для расчета разветвленных и комбинированных конструкций. Предлагаемые равновесные конечные элементы могут быть использованы для более точного определения напряжений в рассчитываемых конструкциях. Предлагаемая методика может быть использована для построения объемных конечных элементов.

### Литература

1. Зенкевич О. Метод конечных элементов в технике. М.: Мир, 1975. 541 с.
2. Зенкевич О., Морган К. Конечные элементы и аппроксимация. М.: Мир, 1986. 318 с.
3. Галлагер Р. Метод конечных элементов. Основы. М.: Мир, 1984. 428 с.
4. Artioli E., de Miranda S., Lovadina C., Patruno L. A stress/displacement Virtual Element method for plane elasticity problems // Comput. Methods Appl. Mech. Eng. 2017. Vol. 325. Pp. 155–174.
5. Чернышева Н.В., Колосова Г.С., Розин Л.А. Пространственные расчеты подземных сооружений с учетом работы окружающего бесконечного массива в однородных и неоднородных областях комбинированным способом // Инженерно-строительный журнал. 2016. № 2(62). С. 83–91.
6. Тюкалов Ю.Я. Улучшенный стержневой конечный элемент для решения задач устойчивости // Инженерно-строительный журнал. 2018. № 3(79). С. 54–65. DOI: 10.18720/MCE.79.6
7. Лалин В.В., Розин Л.А., Кушова Д.А. Вариационная постановка плоской задачи геометрически нелинейного деформирования и устойчивости упругих стержней // Инженерно-строительный журнал. 2013. № 1(36). С. 87–96. DOI: 10.5862/MCE.36.11
8. Artioli E., Miranda S., Lovadina C., Patruno L. A family of virtual element methods for plane elasticity problems based on the Hellinger–Reissner principle // Computer Methods in Applied Mechanics and Engineering. 2018. Vol. 340. Pp. 978–999.
9. Li Z., Chen S., Qu S., Li M. Stabilization of low-order mixed finite elements for the plane elasticity equations // Computers & Mathematics with Applications. 2017. Vol. 73. Pp. 363–373.
10. Leonetti L., Garcea G., Nguyen-Xuan H. A mixed edge-based smoothed finite element method (MES-FEM) for elasticity // Computers & Structures. 2016. Vol. 173. Pp. 123–138.
11. Elakkad A., Bennani M.A., Mekkaoui J., Elkhalfi A. A. Mixed Finite Element Method for Elasticity Problem // International Journal of Advanced Computer Science and Applications. 2013. Vol. 4. No. 2. Pp. 161–166.
12. Мирсаидов М.М., Абдикаримов Р.А., Ватин Н.И., Жгуты В.М., Ходжаев Д.А., Нормуминов Б.А. Нелинейные параметрические колебания вязкоупругой пластинки переменной толщины // Инженерно-строительный журнал. 2018. № 6(82). С. 112–126. DOI: 10.18720/MCE.82.11
13. Сухотерин М.В., Барышников С.О., Кныш Т.П., Абдикаримов Р.А. Собственные колебания прямоугольной пластины, защемленной по двум смежным краям // Инженерно-строительный журнал. 2018. № 6(82). С. 81–94. DOI: 10.18720/MCE.82.8

14. Wang Q., Zhou W., Cheng Y., Ma G., Chang X., Chen E. NE-IIBEFM for problems with body forces: a seamless integration of the boundary type meshfree method and the NURBS boundary in CAD // *Adv. Eng. Softw.* 2018. Vol. 11. Pp. 1–17.
15. Zhou W., Yue Q., Wang Q., Feng Y.T., Chang X. The boundary element method for elasticity problems with concentrated loads based on displacement singular elements // *Engineering Analysis with Boundary Elements.* 2019. Vol. 99. Pp. 195–205.
16. Gu Y., Zhang C., Qu W., Ding J. Investigation on near-boundary solutions for three-dimensional elasticity problems by an advanced BEM // *Int. J. Mech. Sci.* 2018. Vol. 142. Pp. 269–275.
17. Zhou J., Wang K., Li P. A hybrid fundamental-solution-based 8-node element for axisymmetric elasticity problems // *Engineering Analysis with Boundary Elements.* 2019. Vol. 101. Pp. 297–309.
18. Lin Mu, Junping Wang, Xie Ye. A hybridized formulation for the weak Galerkin mixed finite element method // *Journal of Computational and Applied Mathematics.* 2016. Vol. 307. Pp. 335–345.
19. Тюкалов Ю.Я. Конечно элементные модели в напряжениях для изгибаемых пластин // *Инженерно-строительный журнал.* 2018. № 6(82). С. 170–190. DOI: 10.18720/MCE.82.16
20. Тюкалов Ю.Я. Конечно-элементные модели в напряжениях для задач плоской теории упругости // *Инженерно-строительный журнал.* 2018. № 1(77). С. 23–37. DOI: 10.18720/MCE.77.3.
21. Тюкалов Ю.Я. Конечно-элементная модель в напряжениях для пластин Рейснера // *Инженерно-строительный журнал.* 2019. № 5(89). С. 61–78. DOI: 10.18720/MCE.89.6
22. Тюкалов Ю.Я. Метод расчета изгибаемых плит с учетом деформаций сдвига // *Инженерно-строительный журнал.* 2019. № 1(85). С. 107–122. DOI: 10.18720/MCE.85.9
23. Тимошенко С.П., Гудьер Дж. Теория упругости. М.: Наука, 1979. 560 с.

**Контактные данные:**

*Юрий Яковлевич Тюкалов, +7(912)8218977; эл. почта: yutvgu@mail.ru*

© Тюкалов Ю.Я., 2019